# Chapter 11
# Zylon®: Super Fiber from Lyotropic Liquid Crystal of the Most Rigid Polymer

**Yoshihiko Teramoto and Fuyuhiko Kubota**

**Abstract** The research on rigid-rod polybenzazoles (PBZ) was originally intended to develop super fibers for aerospace applications. Due to the technical difficulties in synthesizing PBZ and processing it to fibers, a polybenzoxazole (PBO) fiber, Zylon® launched by Toyobo is the only fiber that has been successfully commercialized so far.

In this chapter, the history of development, manufacturing process, fiber properties, and unique applications are described for Zylon®. Chemistry of PBO and polymerization process are also presented and discussed.

**Keywords** PBO • Polybenzazole • Polycondensation • Liquid crystalline polymer • Dry-jet wet spinning • High-performance fiber • Advanced composite materials • Technical textile • Personal protective equipments • Heat-resistant polymer

## 11.1 History

PBO fiber was commercialized in Japan by Toyobo Company in 1998 [1–6]. Historically, PBO fiber was extensively studied in the USA during the 1980s and 1990s as a next-generation high-performance fiber following aramid fibers. The key synthetic method to achieve high molecular weight in polybenzazole (PBZ) chemistry was to use polyphosphoric acid (PPA) as a solvent as well as a dehydrating agent. The method had been originally developed by Iwakura and Imai in the late 1960s [7–10] and was applied to the synthetic research of ladder polymers and polybenzazoles conducted by the researchers of the US Air Force (USAF) [11]. Chemical structures of typical PBZ polymers are shown in Fig. 11.1.

Kevlar, an aramid fiber, was successfully commercialized by DuPont in 1974. It was an important landmark for high-performance fiber industry. However, even better properties in tensile strength and heat resistance than those of Kevlar were strongly desired, especially for aerospace applications that the USAF people were

Y. Teramoto (✉) • F. Kubota
Research Center, TOYOBO Co., Ltd., 2-1-1 Katata, Otsu, Shiga 520-0292, Japan
e-mail: Yoshihiko_Teramoto@toyobo.jp



Society of F.S. Technology, Japan (ed.), *High-Performance and Specialty Fibers*,
DOI 10.1007/978-4-431-55203-1_11

PDIAB

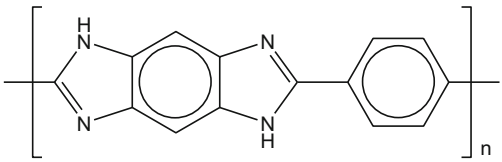


PBO

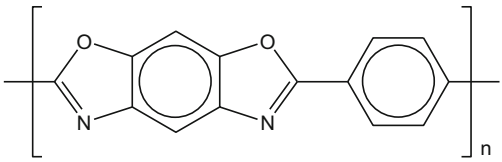


PBZT

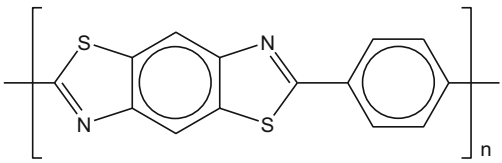


ABPBT

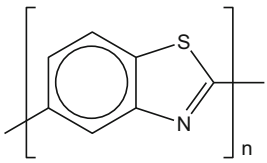


ABPBO

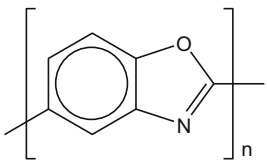


ABPBI

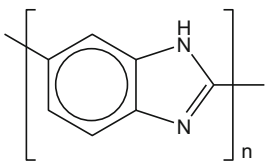


**Fig. 11.1** Chemical structures of typical PBZ polymers

looking at [12]. It drove them to target active works on PBZ, especially *trans*-poly-*p*-phenylene benzobisthiazole (PBZT), which was regarded as the most promising material among PBZ family in terms of solubility of the polymer.

One of the researchers at USAF, Wolfe, moved to Stanford Research Institute (currently SRI International) and further proceeded with the development of PBZ. In PBZ polymerization, $P_2O_5$ content of polyphosphoric acid is the key contributor for achieving a high degree of polymerization. Wolfe et al. designed a systematic way of controlling $P_2O_5$ content during polymerization and successfully obtained fibers that exceed Kevlar® 49 in strength and modulus [13, 14].

In the late 1980s, Dow Chemical was trying to get into the growing market of high-performance fibers. They purchased the patents of PBZ from SRI [15] and started their project covering the whole chemistry and fiber manufacturing. From their commercial point of view, *cis*-poly-*p*-phenylene benzobisoxazole (*cis*-PBO) was more attractive than PBZT, as the monomer for *cis*-PBO, 4,6-diaminoresorcinol (DAR), was expected to be cheaper than those for PBZT. Lysenko et al. developed a new synthetic method for DAR, starting from 1,2,3-trichlorobenzene, which was a big advancement for commercialization of *cis*-PBO fiber [16].

While extensively working on the total process of *cis*-PBO fiber, Dow Chemical realized that it was more efficient to work with a fiber company to accelerate the development. Among several possible options, Dow Chemical picked up Toyobo as their partner, and the joint development started in 1991. Toyobo fiber team made a big contribution to the development of spinning technology, which was quite a big challenge even for fiber specialists, due to the difficulty in spinning resulting from the high rigidity of *cis*-PBO.

In 1994, Dow Chemical made a strategic decision to exit specialty businesses including high-performance fiber business and more focus on their commodity businesses. Under the partnership of joint development for 3 years, Dow Chemical proposed that their technologies for DAR and *cis*-PBO were transferred to Toyobo. Toyobo finally decided to commercialize *cis*-PBO fiber on their own and their polymer team took over Dow's technologies for further developing them in Japan.

In October 1998, Toyobo launched *cis*-PBO fiber, with a trade name of "Zylon®," and started the commercial production in their Tsuruga plant in Fukui, Japan. A Japanese chemical company was a new partner for Toyobo for the DAR monomer supply. It is noteworthy that PBZ chemistry which had been originally developed in Japan finally returned home and bore fruits in the form of "the world's strongest fiber" [1–6].

## 11.2 PBO Chemistry

### *11.2.1 PBZ Chemistry*

PBZ polymers are typically synthesized by polycondensation of AA-type monomers and BB-type monomers. BB-type monomers for *trans*-PBZT and *cis*-PBO are 2,5-diamino-1,4-benzenedithiol dihydrochloride (DABDT) and 4,6-diaminoresorcinol dihydrochloride (DAR), respectively. The AA-type monomer for both is terephthalic acid, and its acid chloride can be used as an alternative as well. PBZ family includes AB-type polymers synthesized by self-condensation of AB-type monomers, but mechanical properties of the resulting fibers are not as good as those of the linear backbone PBZ polymers.

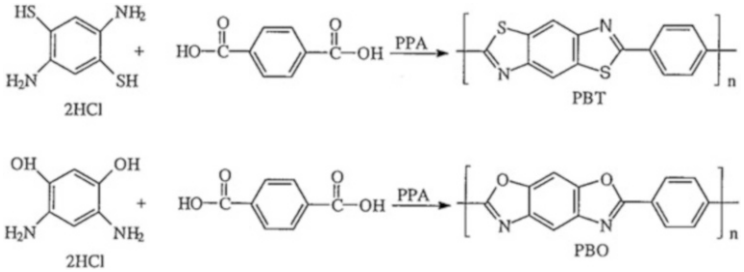


A unique PBZ polymer developed by AkzoNobel in the late 1990s was poly (2,6-diimidazo[4,5-b:4′,5′-e]pyridinylene-1,4-(2,5-dihydroxy)phenylene) (PIPD). The polymer was designed to combine the high stiffness and tenacity of the rigid-rod polymer with possible hydrogen bonding between the polymer backbones. The fiber spun from a polyphosphoric acid solution exhibited a higher compressive strength than any other organic super fiber. The fiber was called M5 in their development stage. The technology had been transferred to Magellan Systems, which DuPont acquired in 2005, to add the new fiber in their lineup of high-performance fibers. However, there has been no further information about commercialization of M5 in DuPont so far.

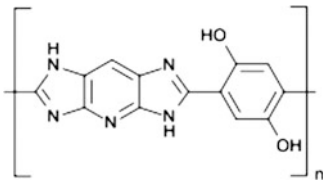

## *11.2.2 PBO Chemistry*

### 11.2.2.1 Monomer Chemistry

The key monomer (BB-type) for *cis*-PBO is 4,6-diaminoresorcinol (DAR). Several starting materials, such as resorcinol and di- or tri-chlorinated benzenes, can be used for the synthesis of DAR. As high purity is required for monomers used in polycondensation, the synthetic route should be well designed to avoid formation of isomers, which may need an additional separation or purification process and lead to lower yield and higher cost.

Wolfe et al. developed a route starting with direct nitration of resorcinol, but the formation of wrong isomer and potential risk of explosive trinitro-byproduct were the issues for scale-up. A novel route starting from 1,2,3-trichlorobenzene (TCB) developed by Lysenko et al. was the first process that could be scaled up for commercialization. As the 2-position of TCB is "protected" by chlorine, there is no possible formation of the wrong isomer and explosive trinitro-byproduct. As a result, high purity can be easily achieved for DAR, although a dechlorination step is required to make the final product.

Alternatively, other routes such as diazotization of resorcinol followed by reduction and nitration of 1,3-dichlorobenzene (DCB) followed by hydrolysis and reduction are also available. However, separation of the isomer could be a challenge to achieve high purity of DAR.

DAR easily undergoes air oxidation, as it has four electron-donating groups in a single benzene ring. In order to avoid degradation through oxidation, DAR has to be handled in the form of acid salt. The most typical salt form is dihydrochloride, which evolves into hydrogen chloride (HCl) gas during the initial stage of polymerization.

Another monomer (AA-type) for *cis*-PBO is terephthalic acid (TA). As solubility of TA in PPA is very low, micronized TA is typically used to enhance the polymerization rate. Alternative AA-type monomer is terephthaloyl chloride, which is more soluble in PPA. However, evolution of HCl gas during the polymerization could be a disadvantage over the simple dehydration in the case of TA.

### 11.2.2.2 Polymerization

As described before, PPA is normally used as a solvent together with $P_2O_5$. Theoretical $P_2O_5$ content in the whole solvent system at the initial stage of polymerization is typically higher than 120 %. The dehydrating power of the solvent system is the driver for polymerization and the $P_2O_5$ content decreases, accordingly as the polymerization proceeds.

When DAR is dissolved in PPA, it readily becomes phosphoric acid salt, while releasing HCl gas. For a process on a commercial scale, evolution of toxic and

corrosive gas can be a big issue. Proper care in handling HCl gas has to be taken for safe and stable operation of the process.

### *11.2.3 Alternative Chemistry for PBO*

While handling of HCl gas is a disadvantage for a commercial process, alternative ways to avoid HCl gas evolution have been investigated. Dow developed a process of using salt of terephthalic acid and DAR (TA/DAR). When TA/DAR is used, it is quite easy to adjust the stoichiometry, for a high degree of polymerization, as the monomer is 1:1 adduct of the two monomers. However, TA/DAR is not stable under air, due to the lower acidity and stabilizing power of terephthalic acid. Therefore, extra care to avoid oxidation has to be taken in handling TA/DAR for the synthetic process and storage.

A unique monomer that can be used for PBO chemistry is a "dimer"-type monomer, whose structure is AA-BB (TA/DAR), covalently bonded DAR and TA. TA/DAR is reasonably stable under air and doesn't have to be any salt. It has the advantages of avoiding HCl gas and of achieving stoichiometry. Therefore, economical synthetic process for the monomer is highly anticipated.

## 11.3 Features of Zylon®

Basic properties of Zylon® (PBO fiber) are shown in Table 11.1. Strength and modulus are almost twice as high as those of poly-*p*-phenylene terephthalamide (PPTA) fiber: as a commercial fiber, Kevlar® and Twaron®. The decomposition temperature of Zylon® is 100 °C higher than that of para-aramid fiber. The limiting oxygen index is 68, which is the highest among organic super fibers. General technical information can be referred in the web page [17]. In spite of the extremely high strength and high modulus, Zylon® can be fabricated into soft fabrics and flexible cords. Zylon® behaves in a different way, unlike general synthetic fibers such as polyester or nylon, in the abrasion resistance test with the metal pins (Fig. 11.2). Abrasion resistance of Zylon® is higher than that of para-aramid fiber under the same load, but much lower than that of ultrahigh-strength polyethylene (PE) fiber.

Expositions of Zylon® have been already published by several experts [4, 18, 19]. In this section, several major properties are described and discussed.

**Table 11.1** Fiber properties of Zylon (PBO fiber)

| | Zylon® AS | Zylon® HM |
|---|---|---|
| Filament decitex | 1.7 | 1.7 |
| Density (g/cm$^3$) | 1.54 | 1.56 |
| Tensile strength | | |
| (cN/dtex) | 37 | 37 |
| (GPa) | 5.8 | 5.8 |
| Tensile modulus | | |
| (cN/dtex) | 1150 | 1720 |
| (GPa) | 180 | 270 |
| Elongation at break (%) | 3.5 | 2.5 |
| Moisture regain (%) | 2.0 | 0.6 |
| Decomposition temperature (°C) | 650 | 650 |
| LOI | 68 | 68 |
| Thermal expansion coefficient | – | $-6 \times 10^{-6}$ |

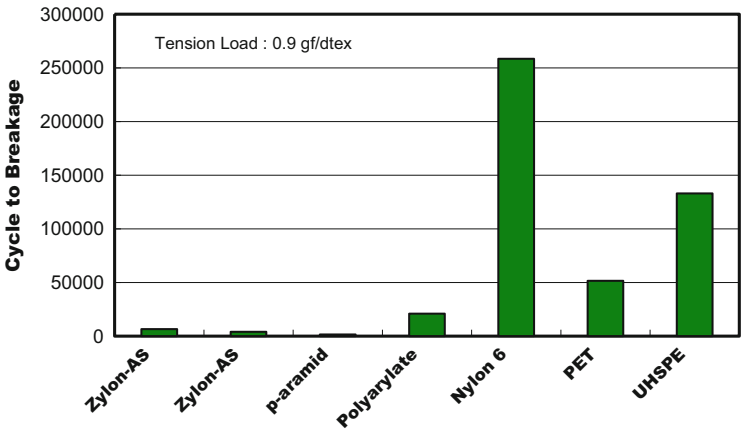


**Fig. 11.2** Abrasion resistance test based on JIS L 1095:1999 9.10.2 B

### *11.3.1 Mechanical Properties*

Stress-strain curves measured for some commercialized high-strength fibers by single filament test are shown in Fig. 11.3. Each curve shows a nearly straight line or a concave line excluding ultrahigh-strength polyethylene (UHSPE) fiber. Ultrahigh-strength PE fiber shows plastic deformation at the normal temperature with high stress in fracture test.

The theoretical strength and Young modulus are listed in Table 11.2.

In the case of high-strength fibers, the measured strength is highly dependent on the gauge length of specimen. In the case of Zylon® AS at gauge length 25 mm, the

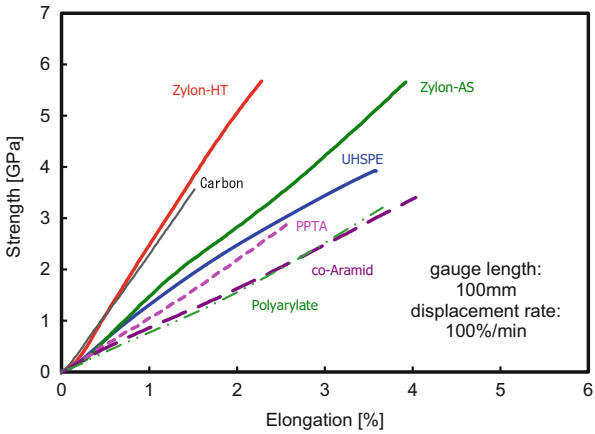


**Fig. 11.3** Stress-strain curves of commercial high-strength fibers

**Table 11.2** Theoretical strength and Young's modulus

| Fiber | Density (g/cm$^3$) | $S^a$ (Å$^2$) | $\sigma c^b$ (GPa) | $Ec^c$ (GPa) |
|---|---|---|---|---|
| Dyneema® [20] | 0.97 | 18.2 | 31 | 235 |
| Kevlar® 49 [20] | 1.44 | 20.2 | 28 | 156 |
| Kevlar® 149 [20] | 1.47 | | | |
| Technora® [20] | 1.39 | 21.0 | 27 | 91 |
| Vectran® [20] | 1.41 | 19.4 | 29 | 126 |
| Zylon® HM [21] | 1.56 | 19.2 | 59 | 690 |

[a] $S$: Effective area for one C-C covalent bond
[b] $\sigma c$: Theoretical strength
[c] $Ec$: Theoretical Young's modulus

mean strength is 7 GPa (Fig. 11.4 [22]). This specification of test method is commonly used for the measurement of carbon fibers. Numbers besides the circles in Fig. 11.4 are shape factor of Weibull distribution. Bigger number means the dispersion of distribution function is small. Filled plots are the mean value of strength with fiber diameter correction. Less than 10 mm gauge length occurrence of end fracture decreases the measurement of strength.

The extrapolation of the slope of −1/14.5 means that the measuring strength will reduce from 7.0 to 6.3 GPa when the gauge length increases from 25 to 250 mm. A 6.3 GPa strength is still higher than the strength measured with multifilament yarn, expecting yarn strength becomes smaller than the strength at average elongation at break of filaments composing the yarn [23]. Therefore, the average strength measured for single filaments is always higher than the strength measured for multifilament yarn.

The modulus of heat-treated Zylon® (type HM) is 270 GPa, which is 40 % of the theoretical estimation and 60 % of the crystalline modulus measured by WAXD [24]. The cause for the difference has not been elucidated directly. Two possible reasons are related to the discussions in the study of PBZ by Lee [25]. The first

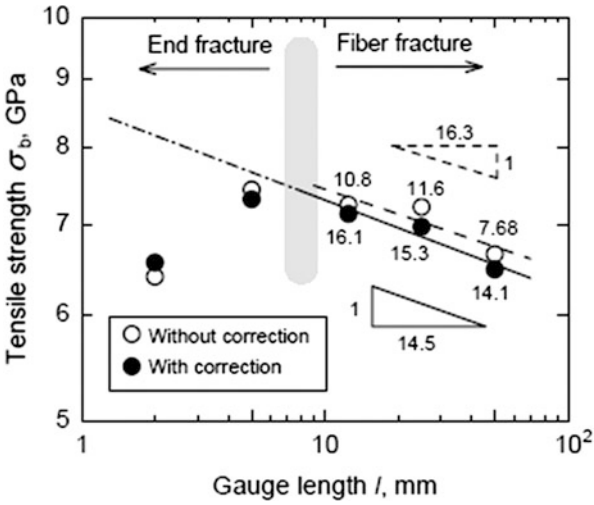


**Fig. 11.4** Specimen length effect on strength for Zylon® AS [22]

possible hypothesis is that large concentration fluctuation during coagulation process disturbs the order in the microfibril structure. The second hypothesis is caused by domain boundaries of liquid crystalline solution structure that is inherent after polymer structure development and behaves as the defect that does not transport stress. Replacement of water with an organic solvent in the coagulation process enhanced modulus of PBO fiber up to 352 GPa [26]. This supports the first mechanism. The differences in the degree of molecular orientations exist between the outer layer and inside of a fiber [27]. This is a phenomenon on several micron scales happening in the coagulation process. Kitagawa et al. applied the mechanical series model that is composed of a series of crystalline domain and low Young's modulus domain. They reported that even in high-modulus heat-treated fiber (Zylon® HM), 14 % fiber volume remains of low modulus [28]. In the structure formation process, the evidence that domain boundary of solution structure is left at coagulation stage has not been reported. But even if domains deform with the large change of aspect ratio, the molecular chain ends tend to concentrate at the boundary. Burger et al. discussed the fine structure to account for the four-point SAXS pattern of PBO-HM [29]. Low density part might be an accumulation of chain ends [30], though. The real image of the area where a Young's modulus is low is still unknown.

### *11.3.2 Compressive Strength*

The anisotropy of the elasticity constants of the PBO fiber (Fig. 11.5) is reported by Yamashita et al. [31]. As shown in Table 11.2, the compression modulus in the lateral direction is small. And the coefficient of PBO fiber is lower than that of PET

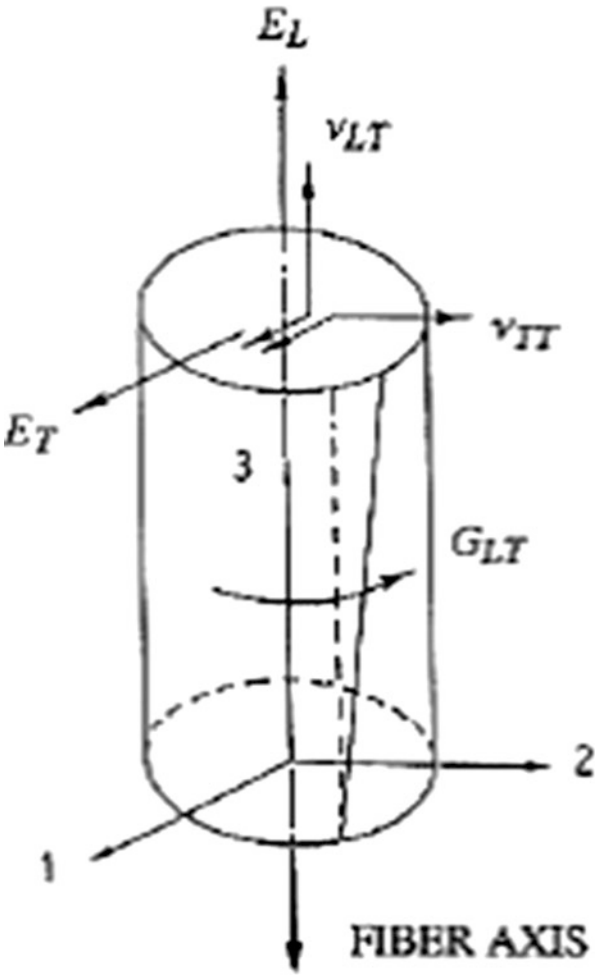


**Fig. 11.5** Definition of nomenclature for elastic constants [31]

fiber. In terms of torsion rigidity, PBO fiber is comparable to PET fiber and is half as rigid as para-aramid (PPTA) fiber. Actually, codes and fabric made of PBO are softer compared with those of PPTAs.

Different methods of measuring the compressive strength of filaments are available, such as elastica loop method, mandrel bending method, bending beam method, and tensile recoil method. These are not direct measurements of stress by axial compressive strain. It is very difficult to apply axial compression for thin filament. So the value of compressive strength in each method is useful for relative comparison between materials. The meaning of compressive strength is usually the load-generating kink bands. This doesn't mean real fracture of a fiber.

Leal et al. compared compressive strength among several high-performance fibers by the elastica loop method [32]. They estimated the ratio of the compressive modulus and the tensile modulus to be 0.32 for PBO fiber. The compressive

**Table 11.3** Elastic constants in Fig. 7.5 for fibers [31]

| Fiber | $E_L$ (GPa) | $E_T$ (GPa) | $G_{LT}$ (GPa) |
|---|---|---|---|
| PBO | 315.2 | 0.91 | 1.02 |
| PPTA (Kevlar® 29) | 79.8 | 2.59 | 2.17 |
| PPTA (Kevlar® 49) | 113.4 | 2.49 | 2.01 |
| Carbon (T-300, PAN) | 234.6 | 6.03 | 18.2 |
| Glass | 77.4 | 67.9 | 42.5 |
| PET | 14.5 | 1.37 | 1.03 |
| Nylon6 | 2.76 | 1.37 | 0.55 |

strength by this evaluation is 0.29 GPa. Assuming the compressive modulus is 73 GPa, the critical strain is about 0.4 %. This value is smaller than 0.56 GPa, which was measured by Toyobo by bending beam method. D$_e$teresa et al. found empirical linear correlation of compressive strength is 30 % of the torsion modulus ($G_{LT}$) [33]. Leal's data of compressive strength are close to 30 % of torsion modulus in Table 11.3.

The crystal structure of PBO was investigated by the X-ray diffraction analysis combined with the computer simulation technique. Planar shape chain forms the sheets with axial shift between the adjacent chains with ±c/4 ($c$ = fiber identity period). Those sheets stack with random shifts along the fiber direction [34, 35]. This structure suggests that PBO crystals include the plane with low interaction to sheer deformation.

Lorenzo-Villafranca et al. defined the limit of compressive strain where fibers deform to V shape. Usually, the limit of compressive strain is judged by discontinuous curvature in elastica loop method. At this compressive strain, kink band is observed, but tensile strength shows no reduction. They call V-shaped damage as "knuckle." Compressive strain where PBO fibers generate "knuckle" is 1.7 %. At this strain tensile strength decreases more than 30 %. This strain is the criteria that fiber would not return to its straight shape. The calculation of the compressive strength greatly varies with the compressive modulus to be applied. In this study, compressive strength was evaluated to be 1.24 GPa. They found plasma treatment under nitrogen improved the compressive strain approximately 40 % [36]. It is interesting that surface treatment on the shell part of a fiber improves compressive strength.

### *11.3.3 Fatigue*

Horikawa et al. analyzed fatigue properties of Zylon® with single filament test for fiber-reinforced composite applications [37]. Under the test condition (12.5 mm gauge length, sinusoidal loading of frequency 10 Hz on three specifications of stress amplitude ratio: $R = 0.1,\ 0.5,\ 0.7$), the breaking life tended to shorten as the maximum stress increases. In addition, the influence of the stress ratio was small. HM type showed longer life than AS type (Fig. 11.6).

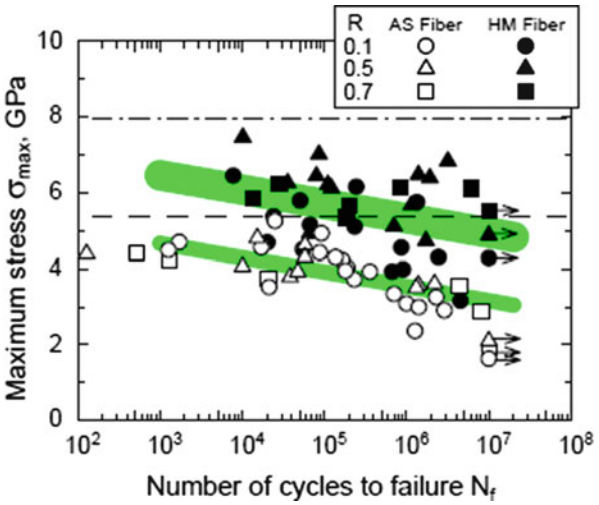


**Fig. 11.6** Cycle number for filament break in single fiber fatigue test [37]. Cutoff cycle is $10^7$. *Bold lines* are least mean square regression for two types of Zylon® fibers. (**a**) PPTA knitted fabric of 2/28 Nm spun yarn. (**b**) PBO knitted fabric of 2/34 Nm spun yarn

### *11.3.4 Flame Resistance*

Having outstanding heat oxidation tolerance and incombustibility as an organic fiber, Zylon® has dramatically improved the performance for the firefighter garment and molten metal protection sheets. Excellent properties of Zylon® such as incombustibility, low smoke emission, high pyrolysis resistance, and high strength made it as the best material for heat- and flame-resistant fabrics [38]. Comparison between Zylon® and para-aramid fibers was made by cone calorimeter examination (ASTM E 1354-90) including HRR (heat release rate), THE (total heat evolved), and FIGRA (fire growth rate) index. In Fig. 11.7 remarkable differences can be observed in terms of the ignition times, the HRRs, and residue of materials [39].

### *11.3.5 Thermal Conductivity*

Fujisiro et al. reported thermal conductivity data of PBO fiber and ultrahigh-strength PE fiber [40]. Recently, Wang reported fiber axial directional thermal conductivities measured by the high time-resolution unsteady-state heat conduction system with heating a part of cross section of single filament (Fig. 11.8). Thermal conductivities of 19 $Wm^{-1}K^{-1}$ and 23 $Wm^{-1}K^{-1}$ were reported for Zylon® HM and Zylon® AS, respectively [41]. As thermal conductivity helps release heat from the fabric, higher conductivity may give favorable results in cone calorimeter examination.

In materials, heat transfer is carried out by electrons or phonons which quantize heat vibration. In electric insulating materials, heat is transferred only by phonons, because electron transfer is restricted. Factors affecting phonon transfer reduce

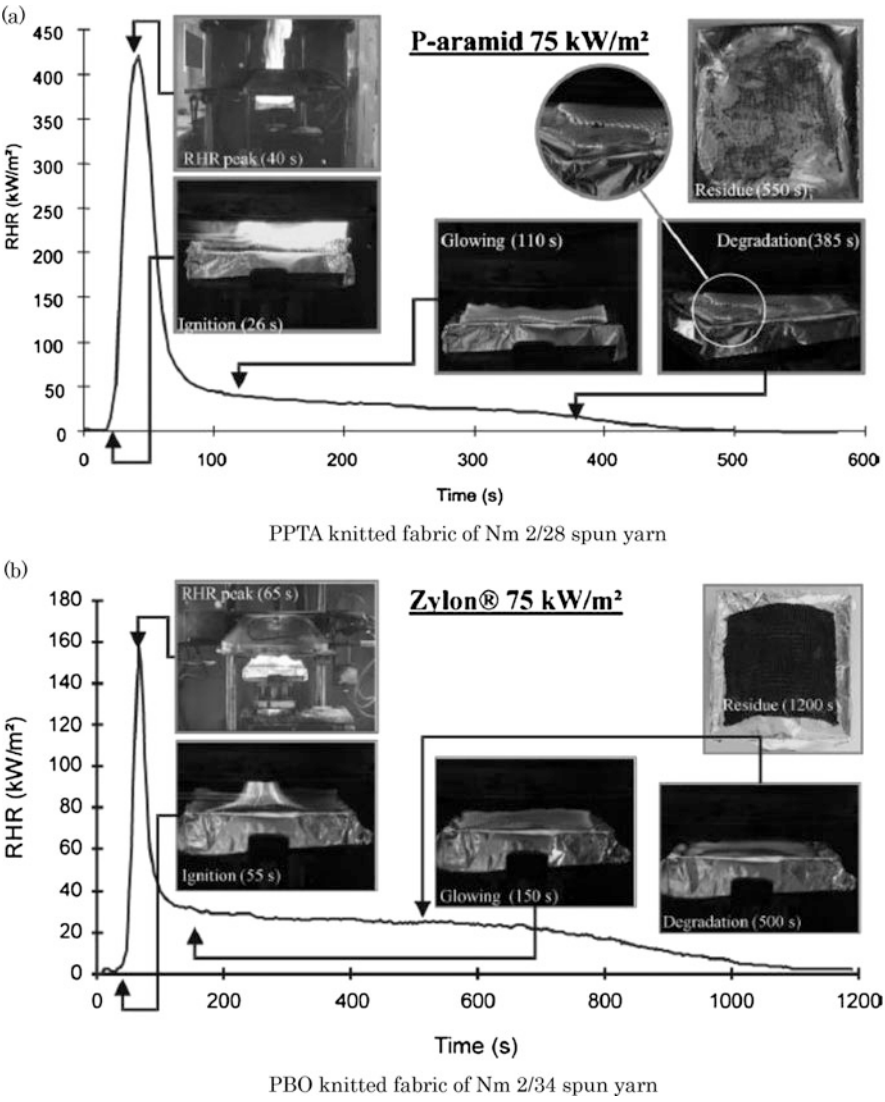


**Fig. 11.7** Cone calorimeter test (ASTM E-1354-90). (**a**) PPTA, (**b**) Zylon® [39]. Surface weight 1.08 kg/m$^2$ knitted samples

thermal conductivity. Molecular chain ends, crystal domain boundaries, mass difference within the units of a macromolecule, and defective placement of molecular chains such as folds and dislocations can scatter phonon propagation. These factors are all similar to defects that reduce fiber strength. It is thought that Zylon® and ultrahigh-strength PE fiber show very high thermal conductivity because of two prerequisites. Firstly, their strength is very high, that is, the amount of defects, such

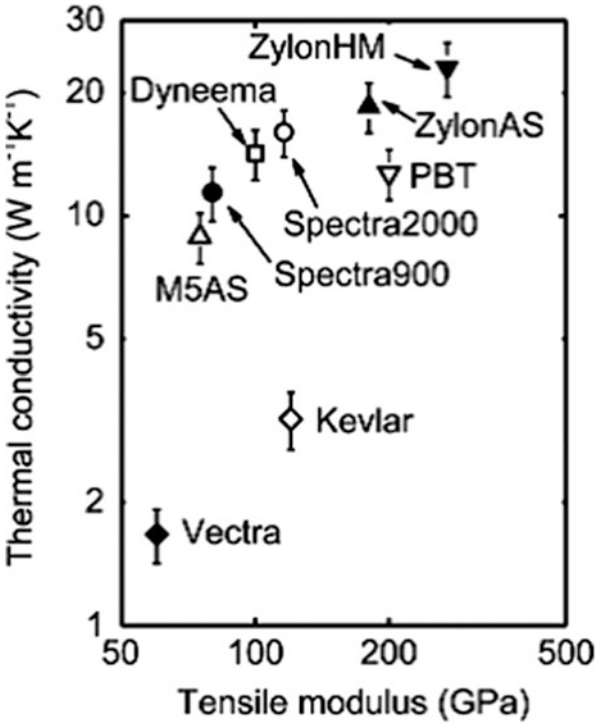


**Fig. 11.8** Room temperature thermal conductivities plotted with tensile modulus [41]

as the chain fold and the chain end, in those fibers is small. Secondly, the polymer structure is suitable for phonon propagation.

Carbonized fiber made from Zylon® HM at a high temperature shows extremely high thermal conductivity. This conductivity exceeds the values of high-modulus-type pitch-based carbon fiber [42]. Kaburagi reported structure analysis of Zylon® HM carbonized graphite. The carbon fiber treated at 3000 °C has a narrow graphite interlayer spacing d002 = 0.3355 nm [43].

### *11.3.6 Degradation Under Hydrolytic Condition*

As polybenzazoles are prepared by dehydration polycondensation, hydrolysis causes breakage of the polymer backbone. So et al. reported the study of intrinsic viscosity (IV) changes during repeated dissolution and reprecipitation of PBO polymer. Firstly, a polymer of IV = 22 was dissolved in methanesulfonic acid containing atmospheric moisture, and then, the polymer was recovered by reprecipitation in water. The IV of the recovered polymer was 15, and no carboxylic acid was detected in its IR spectrum. After repeated operation, carboxylic acid was finally detected, when the IV went down to 2. Meanwhile, when polyphosphoric

acid was used as a solvent, the polymer behaved in a different way. After four times of reprecipitation, the IV dropped from 22 to 5.4 and the carboxylic acid was detected in its IR spectrum [44]. The IV difference was big until the step when amide linkages were cut after oxazole rings were hydrolyzed to amide linkage.

Fiber surface modifications were studied with strong acid [45]. A methanesulfonic acid treatment had a bigger change in surface free energy than a nitric acid treatment. It was shown that surface treatments by acid liquid produced functional group by hydrolysis. This kind of surface treatment is useful as well as plasma treatment.

Chin et al. studied strength drop in a high-temperature and high-humidity environment. Woven PBO fabrics were stored in 50 °C 37 RH% for 84 days and then in 60 °C 60 RH% for 73 days. Fiber strength dropped as the peak of oxazole ring weakened in IR spectrum [46]. Hydrolysis from benzoxazole to benzamide also affects the affinity to moisture. Strength retention data of Zylon® AS for 40 °C 80 RH% aging are disclosed in Toyobo technical information web page [17].

### *11.3.7 Photoaging*

Photoaging is a common phenomenon that can be seen for polymeric materials. Exposure to sunlight can change their chemical, physical, and mechanical properties and such degradation may limit the scope of applications.

The strength of PBO fiber decreases with exposure to sunlight. In the case of Zylon®, photoresistance was evaluated by the use of xenon weather meter. The strength decreased sharply at the initial stage of exposure and the residual strength after 6 months exposure to daylight was about 35 % [17].

There have been several approaches to improve photoresistance of PBO fibers. Zhang et al. coated the fiber surface with zinc nanoparticles/epoxy and found that the tensile strength of coated fiber less declined than that of non-coated fiber under UV irradiation. Shielding effect of the coating layer seems to work to enhance the photostability [47]. Another approach, which is based on chemical modification of the polymer backbone, was proposed by Zhang [48]. Introduction of two hydroxyl groups on the benzene ring of PBO significantly improved UV resistance of the fiber, compared with regular PBO fiber. They suggested that the intermolecular hydrogen bonds play a primary role to improve the UV resistance, avoiding disruption of the oxazole ring, which triggers the degradation of PBO.

Although many efforts have been made so far to understand photoaging mechanism [49–51] and improve photoresistance of a PBO fiber, it is still a big challenge to make it an intrinsically photostable fiber. From a practical point of view, PBO fiber has been used in many applications where the fiber is not exposed to sunlight directly, or decline of strength is not an issue, while heat resistance is mainly appreciated.

## 11.4 Fiber Processing

The process in which polymerized polymer solution was directly used for fiber spinning had been developed by Celanese company [52]. The solvent for fiber spinning is polyphosphoric acid. The difficulties in using polyphosphoric acid solution as spinning dope are as follows, especially complex flow of the nematic liquid crystal solution of rigid-rod polymer ("flow instability"), pretty high viscosity of the polyphosphoric acid solution, and the corrosion of metals by polyphosphoric acid. These three drawbacks make the industrialization very difficult as well as the development of basic production technologies.

As shown in Fig. 11.9, the spinning process for Zylon® consists of the six steps:

1. Extruding the polymer dope of the nematic liquid crystalline phase through capillaries to form filaments (extrusion)
2. Stretching the filaments to make them thinner (spin-drawing)

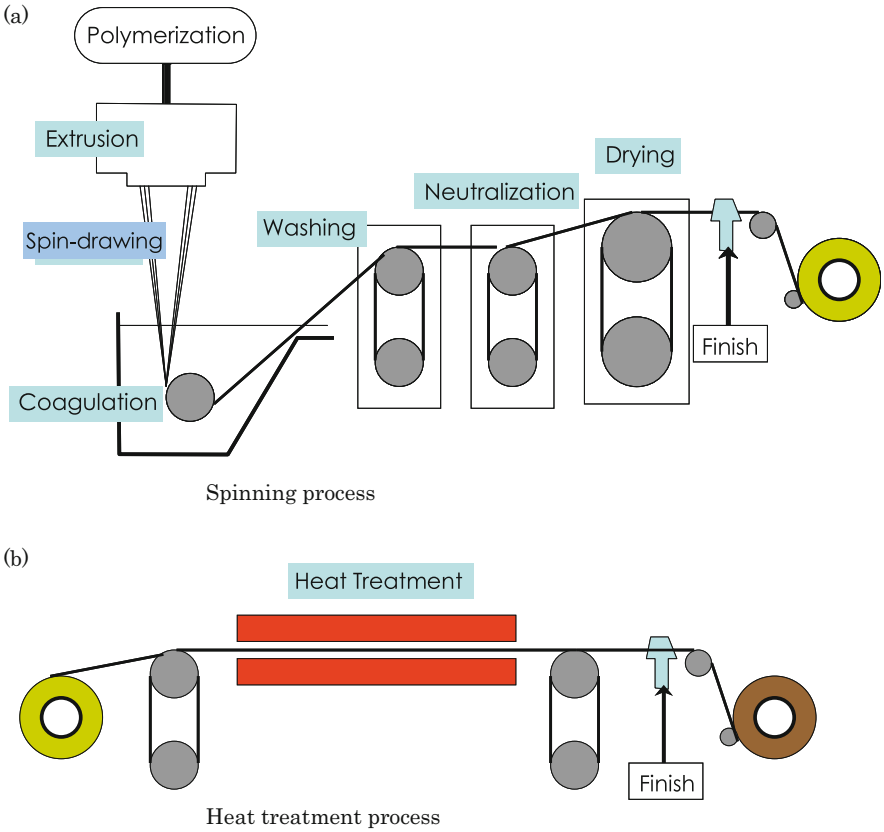


**Fig. 11.9** Fiber production process. (**a**) Setup of spinning sequence consists of six steps. (**b**) Tension and temperature above 450 °C are applied on the heat treatment process

3. Immersing the small-diameter filaments in a non-solvent bath to solidify the fibers (coagulation)
4. Extracting the solvent from the fibers with water (washing)
5. Neutralizing the acid solvent in the fiber with basic solution (neutralization)
6. Drying the fibers (drying)

For the production of high modulus with small moisture regain-type HM fiber, post heat treatment process is necessary, and AS-type fiber is tensed at high-temperature conditions above 450 °C [29].

### *11.4.1 Spinning Dope*

A PBO polymer solution in polyphosphoric acid (10–15 % concentration by weight) is assumed to form the polydomain structure (Fig. 11.10). Due to the poor optical transparency of polymer solution, the optical observation is difficult. Therefore, Odell et al. studied the relaxation of molecular orientation after shear deformations by X-ray diffraction method [53]. The PBZT/PPA = 9.8/90.2 solution (polymer IV = 31 dL/g) at 80 °C between gaps of 50–100 μm for enough time, then stopped shear deformation. One-hundred twenty seconds after ceasing flow, the orientation of polyphosphoric acid relaxed and it took 20 min to relax rigid-rod PBZT molecules. As polyphosphoric acid is an oligomeric material, the flow-induced orientation of polyphosphoric acid molecules can be also observed. However, the 116 % polyphosphoric acid contains more than 40 % chain-formed phosphoric acid molecules which are longer than a heptamer (Fig. 11.11), and the relaxation of orientation of PPA easily occurs. The relaxation of oriented PBZT polymer chain is quite slow in this system.

**Fig. 11.10** Schematic image of polydomain structure

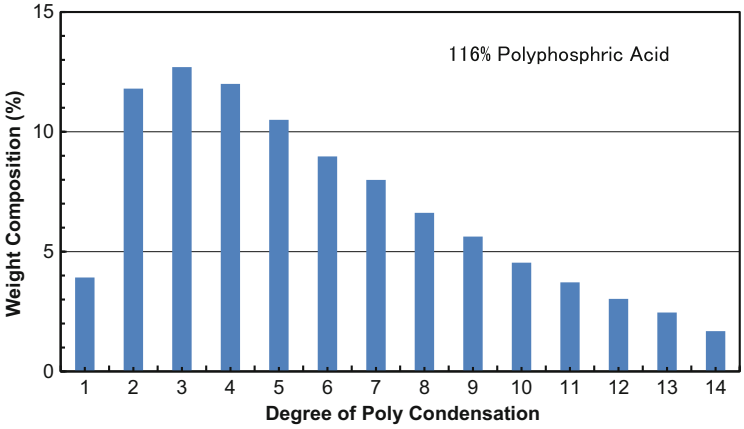


**Fig. 11.11** Polycondensation of polyphosphoric acid [54]

The rheological properties of the rig-rod polymer solution complexity fluids those cause easily the flow instability. When the dope is extruded from a tube at slow flow rate, the millimeter-sized texture is observed on the surface of dope. This is considered to be the trace of the shear flow field at the wall surface accompanying secondary flow. This nature of the dope makes the fiber spinning process difficult.

Ernst et al. studied the coefficient of viscosity of the polyphosphoric acid solution of PBO polymer concentration higher than 10 % suitable for fiber spinning. They compared complex viscosity and steady shear viscosity. The complex viscosity was measured by the linear viscoelastic measurement. The steady shear viscosity at low shear rate was measured by the rotary rheometer. Shear viscosity at high shear rate was measured by a capillary rheometer. Three viscosities were in the same line. This means Cox-Merz's empirical rule was applicable [55]. The lyotropic liquid crystal has characteristic of shear thinning. Viscosity greatly decreases at high shear rate. The complex viscosity of 1000 $s^{-1}$ at 150 °C is approximately 100 Pa.s. On the other hand, the viscosity of PPTA spinning solution of sulfuric acid is some 20 Pa.s by the steady shear viscosity of 1000 $s^{-1}$ at 83 °C [56]. The viscosity of PBO spinning dope is several times higher than that of PPTA spinning dope. Figure 11.12 shows the linear viscoelastic data that were collected at Yamagata University. Temperature to time conversion is valid in the temperature range from 140 to 185 °C. In this temperature range, spinning dope composition stays in nematic phase without solid portion. Shear viscosity data from 24 to 6100 $s^{-1}$ were measured by a capillary rheometer eliminating entry pressure drop from Bagley plot. These data were consistent with the complex viscosity data.

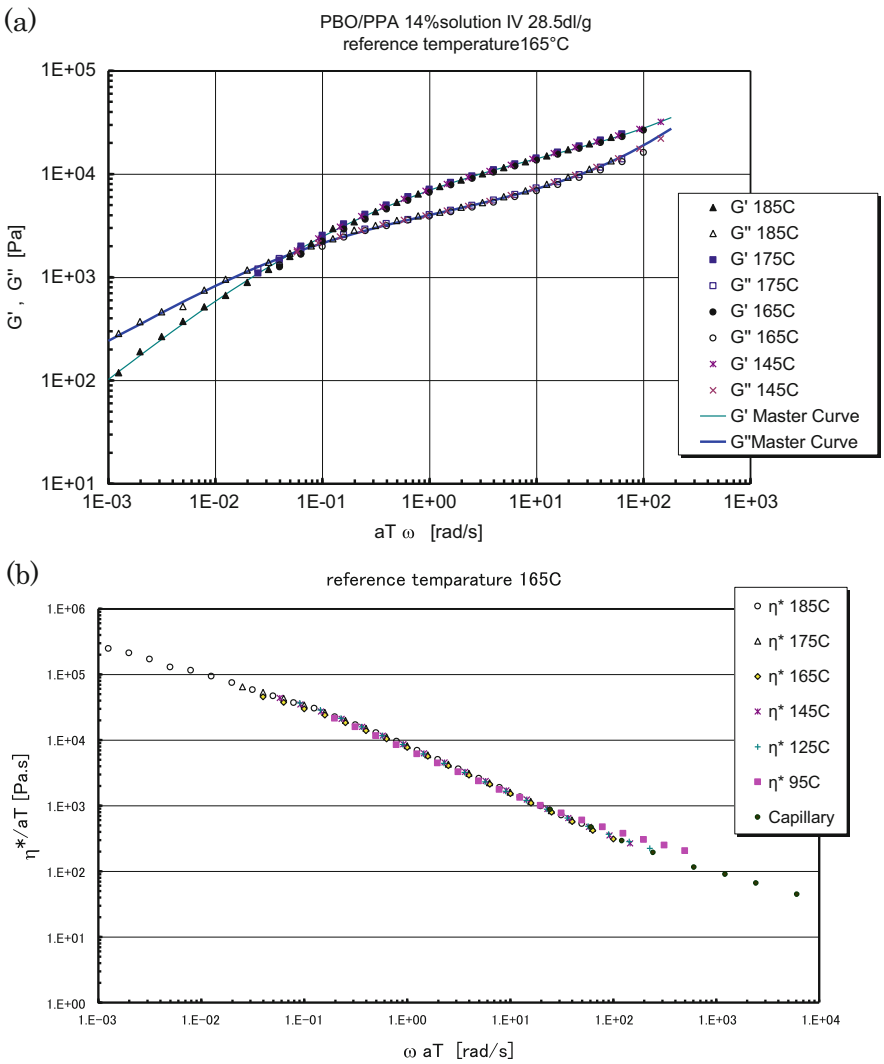


**Fig. 11.12** Linear viscoelastic data of PBO/PPA solution. (**a**) Storage modulus (G′) and loss modulus (G″). (**b**) Complex viscosity. Parallel plate, sample thickness 0.8 mm; strain amplitude 10 %

## *11.4.2 Fiber Processing*

### 11.4.2.1 Spin-Drawing

The spinning dope for PBO fiber is extruded from a capillary and stretched in the air gap. The polymer rods are aligned to axial direction during this process. Researchers of Dow set up a compact spinning line at the synchrotron radiation

X-ray source of the Cornell University. They analyzed the orientation parameter using the equatorial [100] (10.6 Å) reflection peak and the coherence length using equatorial [100] peak and meridian [002] layer line (Fig. 11.13 [57]). Spin-draw ratio (SDR) is defined as winding speed divided by average velocity at the capillary. When the SDR went up to 20, the orientation parameter reached 0.95 and the orientation parameter was almost saturated. The domain size (coherence length) of axial direction calculated from the spread of the [002] peak increased when SDR exceeds 20.

#### 11.4.2.2 Coagulation

Ran et al. reported in situ analyses on the structure formation in the coagulation process. A 240 μm diameter filament of 14 % polyphosphoric acid solution was used for the analysis. At the time of 2 s after dipping in the water bath, there was no big change in the scattering pattern both of WAXD and SAXS. During this coagulation time, the portion that had developed fiber structure was little [58]. The swollen microfibrillar network structure which is proposed by Martin and Thomas [59] would appear later, when most of the phosphoric acid is removed from the fiber. Ran et al. reported a follow-up analysis. At 0.3 s of coagulation, the [010] reflection as the cohesion of the polymer appeared at the fiber surface [60]. Daves et al. proposed a structure development model, which generated crystals at the fiber surface regulating the lattice direction of [010] plain and increasing toward the inner part of the fiber [61]. At present, there is no evidence we can ascertain as to whether or not molecules in solution are oriented radially before coagulation. Preferential orientation of PBO fiber was reported as the *a*-axis of crystal lined up in radial direction [29].

#### 11.4.2.3 Washing and Neutralization

The fiber swelled with water is formed after polyphosphoric acid is extracted from the stretched solution filament. The volume fraction of the water in this soaked fiber is approximately 50 %. The phosphoric acid can be extracted rapidly in a state containing enough amount of water. Approximately 0.6 % of phosphoric acid stays in fibers even after a prolonged extraction time. Phosphoric acid molecule coordinates to an amino phenol end group or to an oxazole ring, and such a “trapped” phosphoric acid is not easy to extract by washing and stays in the fiber as a residual acid [62]. The washed fiber is soaked in an alkaline water to neutralize the residual phosphoric acid.

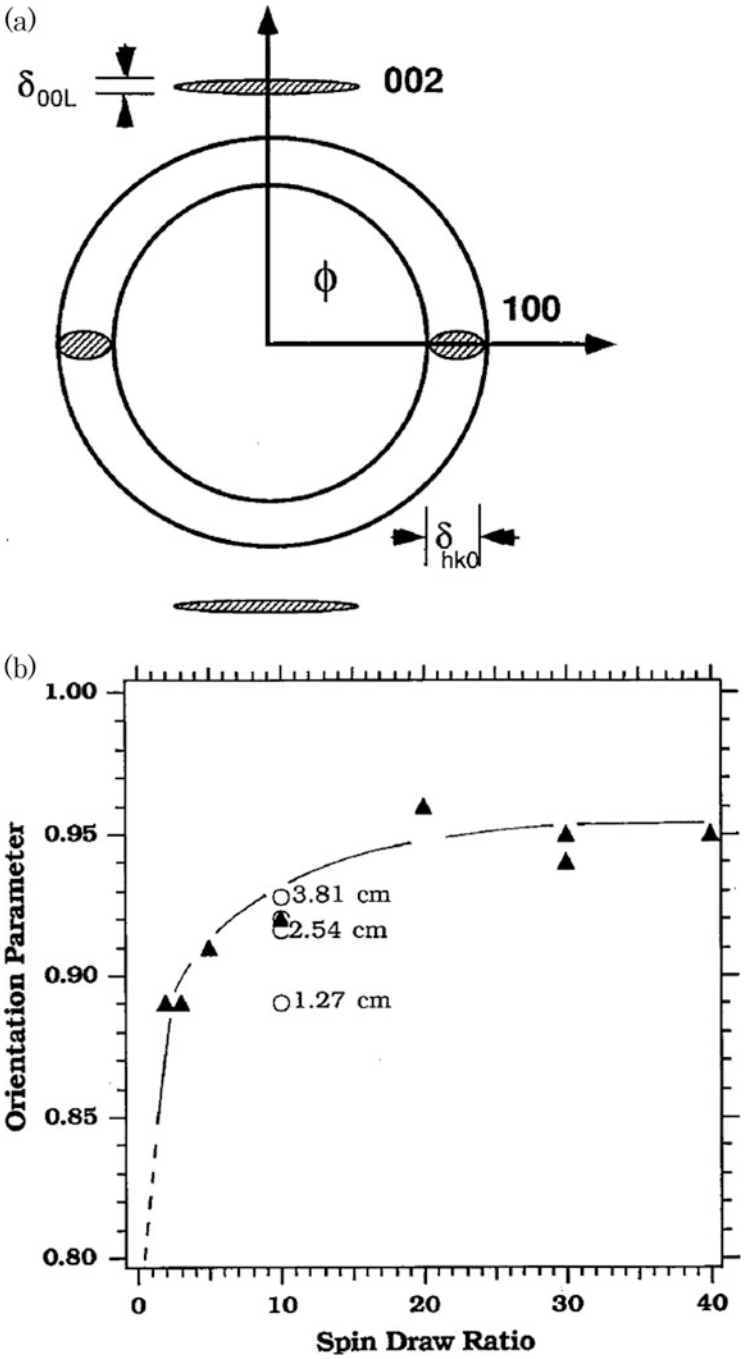


**Fig. 11.13** In situ WAXD analysis of PBO/PPA solution spinning [57]. (**a**) Principal diffraction spots. (**b**) Orientation development in spin line

#### 11.4.2.4 Drying

The moisture content of the washed fiber can reach an equilibrium moisture content, even if the fiber is simply left under normal ambient atmosphere. The modulus of dried fiber, reflecting the orientation degree of the molecules, can be changed by controlling tension and temperature during the drying process [63].

## 11.5 Applications

Having an extremely high performance as a novel super fiber, Zylon® has explored a lot of applications during the last 15 years, since it was launched in 1998. Its applications are categorized into three groups.

### *11.5.1 Heat-Resistant Materials*

Zylon® is used in industrial materials and personal protective equipment (PPE). For these applications, its excellent mechanical strength is highly appreciated, in addition to its superior properties such as heat dissipation, flame resistance, and heat resistance. Examples of application for industrial materials are cushions used in extrusion process of aluminum materials, cushions for processing heated glasses, and protective materials against sputtered metals for welding robots in car production lines. Major applications for PPE are garment and accessories for firefighters and protective materials used in metal manufacturing process and metal welding work.

### *11.5.2 Fiber-Reinforced Composites*

The fiber reinforcements using Zylon® are intended to utilize its tensile properties (strength and modulus) or its abrasion resistance. In the former case, Zylon® is used for carbon fiber-reinforced plastics to improve fracture toughness and retain configurations at crash destruction. Some Formula One cars have introduced a chassis of carbon fiber-reinforced plastics hybridized with Zylon®. The materials reinforced with Zylon® show superior penetration resistance (Fig. 11.14). Zylon® is used for high-end applications requiring high specifications, such as racing helmets and turbine containment.

In the latter case, the very high abrasion resistance of Zylon® is appreciated, as the abrasion wear is minor, when the cross sections of fibers are rubbed by metals. The life of the rubber belts for continuously variable transmission (CVT) improves

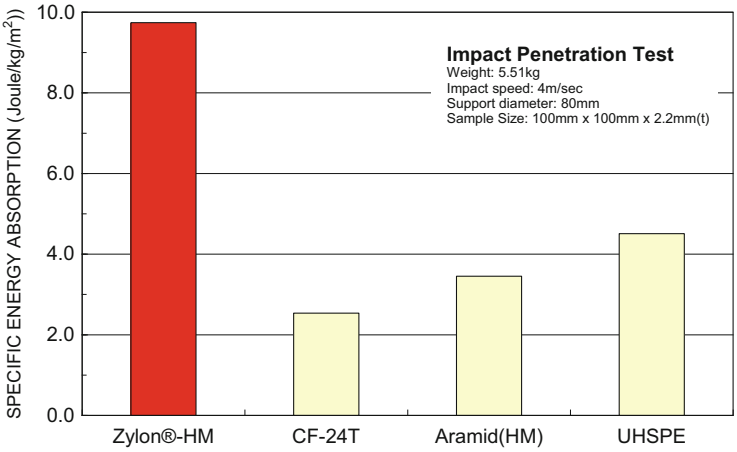


**Fig. 11.14** Impact penetration property

a lot, when Zylon® chopped fibers are added to the rubber as fillers. The Zylon® filler is used in CVTs for motorcycles and snowmobiles.

### *11.5.3 Rope and Cables*

There are two unique applications where Zylon® is used as a tether for safety in racing cars and space exploration vehicles. In 1999, Formula One World Championship started to take safety measures to avoid accidents caused by scatter of suspension parts of crashed cars. Since then, Zylon® has been used for tethers tying monocoque bodies and suspensions or uprights.

Another interesting application is for Mars Exploration Rover (MER). In 2004, NASA successfully landed a MER on Mars. For a smooth and safe landing, the rocket and the rover were tied with a tether to control the posture of the three bodies (Rover wrapped by air bags, solid rocket motor, and parachute). Zylon® was used for this tether application, due to the highest properties in strength and heat resistance among the super fibers existing on the earth [64].

Zylon® has been used for a lot of sports goods so far, such as tennis rackets, table tennis rackets, and strings for the Japanese art of archery, "wakyu." Another unique example is a tire or wheel for bicycles. Spinergy company commercialized a lightweight wheel for racing bicycles [65], in which metal spokes have been replaced by Zylon® spokes (Fig. 11.15). Figure 11.16 shows creep properties with safety factor 2 (50 % load of the break). Such excellent creep resistance will further realize even more unique applications.


**Fig. 11.15** Zylon spokes for racing bicycle [65]

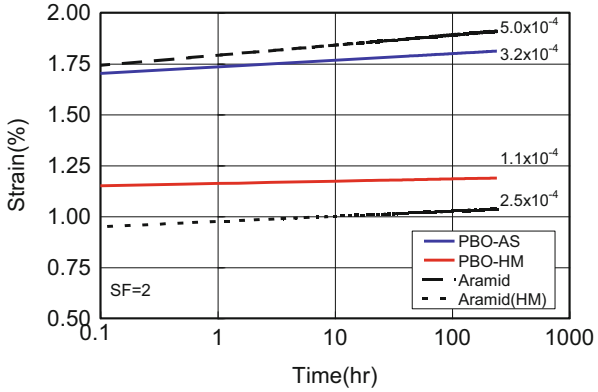


**Fig. 11.16** Creep parameters of PBO (Zylon®) and *p*-aramid (PPTA)

## 11.6 Conclusions

Many researchers and engineers in universities, USAF, SRI, Dow Chemical, and Toyobo contributed to the birth of the world's strongest fiber. It is noteworthy that each party played a different key role at a different stage, and the total development finally bore fruits under the continuous "teamwork" performed over 20 years.

As described and discussed in this chapter, Zylon® has outstanding characteristics in strength, modulus, flame resistance, creep resistance, and thermal

conductivity among the existing organic fibers. However, high-strength fibers have the tendency to be affected by the defect formed by various deterioration modes, as they have very few defects before use. Further efforts to control defect generation will make Zylon® more useful and attractive in the existing applications and will also open a door for new applications. Meanwhile, for applications where heat resistance is appreciated, further development to improve the performance targeting inorganic materials is highly anticipated.

## References


1. K. Yabuki, K. Kato, Sen'i Gakkaishi J. **52**, 143 (1996)
2. T. Kuroki, K. Yabuki, Sen'i Gakkaishi J. **54**, 16 (1998)
3. K. Kato, Kobunshi J. **48**, 20 (1999)
4. K. Yabuki, in *Progress in Textiles: Science and Technology*, ed. by V.V. Kothari, vol. 2 (IAFL Publications, New Delhi, 2000), pp. 615–651
5. F. Kubota, Kobunshi J. **54**, 246 (2005)
6. Y. Imai, Sen'i Gakkaishi J. **61**, 278 (2005)
7. Y. Iwakura, K. Uno, Y. Imai, J. Polym. Sci. Part A: Polym. Chem. Macromol. Chem. **2**, 2605 (1964)
8. S. Inoue, Y. Imai, K. Uno, Y. Iwakura, Macromol. Chem. **95**, 236 (1966)
9. Y. Iwakura, Kobunshi J. **17**, 130 (1968)
10. Y. Imai, Kobunshi J. **20**, 510 (1971)
11. D.R. Ulrich, Polymer **28**, 533 (1987)
12. F.E. Arnold, Mater. Res. Soc. Symp. Proc. **134**, 75 (1989)
13. J.F. Wolfe, Mater. Res. Soc. Symp. Proc. **134**, 253 (1989)
14. J.F. Wolfe et al., Macromolecules **14**, 1135 (1981)
15. SRI U.S. Patent, 4,225,700, U.S. Patent, 4,533,724, U.S. Patent, 4,533,692, U.S. Patent, 4,533,693, U.S. Patent, 4,545,232
16. Z. Lysenko, U.S. Patent, 4,766,244
17. http://www.toyobo-global.com/seihin/kc/pbo/Technical_Information_2005.pdf
18. H.G. Chae, S. Kumar, J. Appl. Polym. Sci. **100**, 791 (2006)
19. H. Murase, Sen'i Gakkaishi J. **66**, 176 (2010)
20. T. Ito, Polym. Prepr. Jpn. J. **42**, 49 (1993)
21. S.G. Wierschke, Mater. Res. Soc. Symp. Proc. **134**, 313 (1989)
22. N. Horikawa, Y. Nomura, T. Kitagawa, Y. Haruyama, A. Sakaida, T. Imamichi, S. Sasaki, H. Takekawa, Nihon Kikai Gakkai Ronbunshu J. **75**, 373 (2009)
23. Z. Chi, T.-W. Chou, G. Shen, J. Mater. Sci. **19**, 3319 (1984)
24. T. Kitagawa, K. Tashiro, K. Yabuki, J. Polym. Sci. Part B **40**, 1269 (2002)
25. C.Y.-C. Lee, U. Santhosh, Polym. Eng. Sci. **33**, 907 (1993)
26. T. Kitagawa, M. Ishitobi, K. Yabuki, J. Polym. Sci. Part B **38**, 1605 (2000)
27. T. Kiagawa, K. Yabuki, R.J. Young, J. Macromol. Sci. Part B **41**, 1 (2002)
28. T. Kitagawa, K. Tashiro, K. Yabuki, J. Polym. Sci. Part B **40**, 1281 (2002)
29. T. Kitagawa, H. Murase, K. Yabuki, J. Polym. Sci. Part B **36**, 39 (1998)
30. C. Burger, S. Ran, D. Fang, D. Cookson, K. Yabuki, Y. Teramoto, P.M. Cunniff, P.J. Viccaro, B.S. Hsiao, B. Chu, Macromol. Symp. **195**, 297 (2003)
31. Y. Yamashita, S. Kawabata, H. Minami, S. Okada, A. Tanaka, Proceedings of the 30th Textile Research Symposium at Mt. Fuji in the New Millennium, Shizuoka, **219**, (2001)
32. A.A. Leal, J.M. Deitzei, J.W. Gillespie Jr., J. Compos. Mater. **43**, 661 (2009)
33. S.J. Deteresa, R.S. Porter, R.J. Farris, J. Mater. Sci. **23**, 1886 (1998)

34. K. Tashiro, J. Yoshino, T. Kitagawa, H. Murase, K. Yabuki, Macromolecules **31**, 5430 (1998)
35. K. Tashiro, H. Hama, J. Yoshino, Y. Abe, T. Kitagawa, K. Yabuku, J. Polym. Sci. Part B **39**, 1296 (2001)
36. E. Lorenzo-Villafranca, K. Tamargo-Maet¡nez, J.M. Molina-Aldareguia, C. Gonz'alez, A. Mat¡nez-Alonso, J.M.D. Tasc'on, M. Gracia, J. Llorca, J. Appl. Polym. Sci. **123**, 2052 (2012)
37. N. Horikawa, Y. Haruyama, A. Sakaida, M. Ueda, J. Soc. Mater. Sci. Jpn. J. **54**, 801 (2005)
38. S. Bourbigot, X. Flambard, Fire Mater. **26**, 155 (2002)
39. S. Bourbigot, X. Flambard, F. Poutch, S. Duquesne, Polym. Degrad. Stab. **74**, 481 (2001)
40. H. Fujishiro, M. Ikebe, T. Kashima, A. Yamanaka, Jpn. J. Appl. Phys. **36**, 5633 (1997)
41. X. Wang, V. Ho, R.A. Segalman, D.G. Cahill, Macromolecules **46**, 4937 (2013)
42. Japanese Laid-open Patent 2010-144299A
43. Y. Kaburagi, K. Yokoi, A. Yoshida, Y. Hishiyama, TANSO **217**, 111 (2005)
44. Y.-H. So, S.J. Martin, K. Owen, P.B. Smith, C.L. Karas, J. Polym. Sci. Part A **102**, 1428 (1999)
45. G. Wu, C.-H. Hung, S.-J. Liu, ICCM12 Conference, Paris, July 1999, paper 616, ISBN 2-9514526-2-4
46. J. Chin, A. Forster, C. Clerici, L. Sung, M. Oudina, K. Rice, Polym. Degrad. Stab. **92**, 1234 (2007)
47. C.-H. Zhang, Y.-D. Huang, W.-J. Yuan, J.-N. Zhang, J. Appl. Polym.Sci. **120**, 2468 (2011)
48. T. Zhang, J. Jin, S. Yang, G. Li, J. Jiang, J. Polym. Adv. Technol. **22**, 743 (2011)
49. Y.-H. So, J.M. Zaleski, C. Murlick, A. Ellaboudy, Macromolecules **29**, 2783 (1996)
50. Y.-H. So, Polym. Int. **55**, 127 (2006)
51. B. Song, Q. Fu, L. Ying, X. Liu, Q. Zhuang, Z. Han, J. Appl. Polym. Sci. **124**, 1050 (2011)
52. E.C. Chenevey, T.E. Helminiak, U.S. Patent 4,606,875
53. J.A. Odell, G. Ungar, J.L. Efijoo, J. Polym. Sci. Part B **31**, 141 (1993)
54. D.F. Toy, *Comprehensive Inorganic Chemistry* (Pergamon Press, New York, 1973), p. 486
55. B. Ernst, M.M. Denn, P. Pierini, W.E. Rochefort, J. Rheol. **36**, 289 (1992)
56. M. Mortie, P. Moldenaers, J. Mewis, Rheol. Acta **35**, 57 (1996)
57. M.J. Radler, B.G. Landes, S.J. Nolan, C.F. Broomall, T.C. Chritz, P.R. Roudolf, M.E. Mills, R.A. Bubeck, J. Polym. Sci. Part B **32**, 2567 (1994)
58. S. Ran, C. Burger, D. Fang, X. Zong, S. Cruz, B. Chu, B.S. Hsiao, R.A. Bubeck, K. Yabuki, Y. Teramoto, D.C. Martin, M.A. Johnson, P.M. Cunniff, Macromolecules **35**, 433 (2002)
59. D.C. Martin, E.L. Thomas, Mater. Res. Soc. Symp. Proc. **134**, 415 (1989)
60. S. Ran, C. Burger, D. Fang, X. Zong, S. Cruz, B. Chu, B.S. Hsiao, Y. Ohta, K. Yabuki, P.M. Cunniff, Macromolecules **35**, 9851 (2002)
61. R.J. Davies, M. Burghammer, C. Riekel, Macromolecules **40**, 5038 (2007)
62. N.V. Lukasheva, Polymer **52**, 1458 (2011)
63. M.E. Mills et. al., U.S. Patent 5,976,447
64. http://marsrover.nasa.gov/mission/spacecraft_edl_parachute.html
65. http://www.spinergy.com